Numerical Study of Microwave Reflectometry in Plasmas with 2D Turbulent Fluctuations

E. Mazzucato

Princeton Plasma Physics Laboratory, P.O. Box 451, Princeton, New Jersey 08543

This paper describes a numerical study of the role played by 2D turbulent fluctuations in microwave reflectometry – a radar technique for density measurements using the reflection of electromagnetic waves from a plasma cutoff. The results indicate that, if the amplitude of fluctuations is below a threshold which is set by the spectrum of poloidal wavenumbers, the measured backward field appears to originate from a virtual location behind the reflecting layer, and to arise from the phase modulation of the probing wave, with an amplitude given by 1D geometric optics. These results suggest a possible scheme for turbulence measurements in tokamaks, where the backward field is collected with a wide aperture antenna, and the virtual reflecting layer is imaged onto the plane of an array of detectors. Such a scheme should be capable of providing additional information on the nature of the short-scale turbulence observed in tokamaks, which still remains one of the unresolved issues in fusion research.

I. INTRODUCTION

Microwave reflectometry, an offspring of methods used in ionospheric studies,[1] is extensively used in tokamak research for the measurement of plasma density. Since the original proposal of employing FM-CW radar techniques in combination with swept millimeter-wave oscillators,[2,3] microwave reflectometry has matured quickly to the point of being seriously considered for plasma density measurements in a fusion reactor.[4-7] Indeed, the modest requirement for plasma accessibility and the possibility of conveying microwaves to a remote location make reflectometry an ideal method for the hostile environment of a fusion reactor.

In microwave reflectometry, the plasma density is inferred from the position of a plasma cutoff, which is determined using the dependence of the phase ϕ of a reflected wave on its frequency ω, i.e., from the round-trip group delay $d\phi(\omega)/d\omega$. From the assumption that $\phi(\omega)$ is given by the geometric optics approximation

$$\phi = 2\frac{\omega}{c}\int_0^{r_c}\sqrt{\varepsilon}\ dr\ ,\qquad(1)$$

and the appropriate initial conditions, it is possible to derive the electron density profile. In Eq. (1), as in the rest of this paper, we assume that a unit amplitude wave is launched parallel to the gradient of the plasma permittivity ε, and we denote with r a radial coordinate, and with r_c the location of the reflecting cutoff.

The presence of turbulent fluctuations may severely increase the difficulty of inferring the average electron density profile from reflectometry measurements. On the other hand, this technique is one of the best available tools for the measurement of fluctuations in the main core of tokamak plasmas, and for the study of the role of turbulence in the process of anomalous transport. In fact, the first evidence for the existence of a short-scale turbulence in tokamak plasmas was provided by the first application of this technique to fusion research.[8]

In the presence of density fluctuations, the interpretation of reflectometry measurements is relatively simple when the plasma permittivity varies only along the direction of propagation of the probing wave. This can be seen by taking a plasma permittivity in the form $\varepsilon = \varepsilon_0(r) + \tilde{\varepsilon}(r)$ (where $\tilde{\varepsilon}(r)$ is the contribution of fluctuations), and by assuming that $|\tilde{\varepsilon}| \ll 1$. The wave equation can then be solved with the method of successive approximations. Apart from a constant phase, the first order term (Born approximation) outside of the plasma is given by[9-12]

$$E_1 = 2k_0\exp(ik_0 r)\int_0^\infty \tilde{\varepsilon}(z)A^2(z)dz\ ,\qquad(2)$$

where $k_0 = \omega/c$ is the vacuum wavenumber, and $A(r)$ is a zero order solution of the wave equation with $A(r)\to 0$ for $r\to\infty$, and $A(r)\to\cos(k_0 r)$ for $r\to 0$. When $\varepsilon_0(r)$ is a linear function, both $A(r)$ and the zero order field E_0 become, apart from a constant factor, the Airy function Ai. When $|E_1| \ll |E_0|$, Eq. (2)

is a good approximation of the total scattered field. Under these conditions, by casting the backward wave in the form $\exp(ik_0 r) + i\phi$, from Eq. (2) we obtain that the contribution of fluctuations to the phase of the reflected wave is

$$\tilde{\phi} = 2k_0 \int_0^\infty \tilde{\varepsilon}(r) A^2(r) dr .$$ (3)

On the other hand, by expanding $\sqrt{\varepsilon}$ to the first order in $\tilde{\varepsilon}$, from Eq. (1) we get

$$\tilde{\phi} = k_0 \int_0^{rc} \frac{\tilde{\varepsilon}}{\sqrt{\varepsilon_0}} dr .$$ (4)

Away from the cutoff, where $A(r) \approx \varepsilon_0^{-1/4} \cos(k_0 \int_0^r \sqrt{\varepsilon_0(z)} dz - \pi/4)$ (WKBJ approximation[1]), the coefficient of $\tilde{\varepsilon}$ in the integrand of Eq. (4) is the average over a distance $\Delta r = \pi / k_0 \varepsilon_0^{1/2}$ of the similar coefficient in Eq. (3). This is not true near the cutoff where $\varepsilon_0^{-1/2} \to \infty$ and $A^2 \propto Ai^2(\zeta)$, with $\zeta \equiv (\omega^2 / c^2 L_\varepsilon)^{1/3}(r_c - r)$ and $L_\varepsilon^{-1} = (d\varepsilon_0 / dr)_{r=r_c}$. Since the WKBJ approximation is valid up to the last lobe of $A^2(\zeta)$, which near $\zeta \approx 0$ has a width of $\Delta\zeta \approx 3$ (i.e., $\Delta r \approx 3(k_0 L_\varepsilon)^{1/3} / k_0$), we conclude that Eq. (4) represents a good phase approximation when fluctuations have a radial wavenumber in the range $|k_r| < k_G \equiv \pi / \Delta r \approx k_0 / (k_0 L_\varepsilon)^{1/3}$, so that the scattered field is strongly weighted by fluctuations near the cutoff. On the contrary, when $|k_r| >> k_G$, the scattered field may originate from fluctuations located away from the cutoff where the spatial variation of $A^2(r)$ matches that of the density perturbation (Bragg resonance condition).[10-12]

For $|k_r| < k_G$, using $\varepsilon_0(r) \approx (r_c - r) / L_\varepsilon$ in Eq. (4) we obtain[13]

$$\Gamma_\phi(k_r) = 2\pi \frac{k_0^2 L_\varepsilon}{|k_r|} [C^2(w) + S^2(w)] \Gamma_\varepsilon(k_r) ,$$ (5)

where $\Gamma_\varepsilon(k_r)$ and $\Gamma_\phi(k_r)$ are the Fourier transforms of the radial correlation of $\tilde{\varepsilon}$ and $\tilde{\phi}$ (considered as a function of r_c), respectively, and $C(w)$ and $S(w)$ are the Fresnel integrals[14] with $w = (2|k_r| L_\varepsilon / \pi)^{1/2}$. For the case of interest in tokamaks, where $w >> 1$, $C(w) \approx S(w) \approx 1/2$, while for $w << 1$, $C(w) \approx w$ and $S(w) \approx 0$.

The interpretation of reflectometry becomes considerably more difficult in the presence of two-dimensional (2D) fluctuations, i.e., when the plasma permittivity varies perpendicular to the direction of propagation of the probing wave. The difficulty persists even when the approximation of geometric

3

optics is applicable. Suppose, for example, that in the system of orthogonal coordinates (r,x), representing the radial and the poloidal directions of a tokamak, the wave permittivity is $\varepsilon = \varepsilon_0(r) + \tilde{\varepsilon}(r,x)$, and that the reflected wave, as in the 1D case, can be cast in the form $\exp(i\tilde{\phi})$, with $\tilde{\phi}(x)$ given by Eq. (1). In a random medium, as in a tokamak plasma where the average density is perturbed by a small-amplitude short-scale turbulence, the phase of the probing wave is the cumulative result of many random contributions, so that it is reasonable to assume that $\tilde{\phi}$ is a normal random variable with mean $<\tilde{\phi}>= 0$, variance $\sigma_\phi^2 \equiv <\tilde{\phi}^2>$ and autocorrelation $\gamma_\phi(\xi) \equiv <\tilde{\phi}_1(x)\tilde{\phi}_2(x+\xi)>/\sigma_\phi^2$. From this, we obtain that the first moment of the wave electric field, which can be interpreted as the amplitude of a coherent specular reflection, is $<E>= \exp(-\sigma_\phi^2/2)$, and thus it is a strong decreasing function of σ_ϕ. For the second moment we get $<E_1 E_2^*>= \exp[-\sigma_\phi^2(1-\gamma_\phi)]$, which proves that the autocorrelation width is also a decreasing functions of σ_ϕ. In particular, for $\sigma_\phi >> 1$, taking $\gamma_\phi(\xi) = \exp[-(\xi/\Delta)^2]$ and expanding to the second order in ξ, we obtain $<E_1 E_2^*>\approx \exp[-(\sigma_\phi \xi/\Delta)^2]$. This proves that in the presence of 2D density fluctuations, the range of wavenumbers of the scattered waves can become broader than the spectrum of $\tilde{\phi}$, and consequently broader that the spectrum of the plasma fluctuations themselves. Under these conditions, it becomes very difficult to infer the properties of plasma fluctuations from reflectometry measurements.[13] The problem becomes even more complicated when the approximation of geometric optics is no longer valid, making microwave reflectometry a useless technique for diagnosing tokamak plasmas.

The assumptions made in the previous paragraph, i.e., that reflectometry consists of a phase modulation of the probing wave, occurring mostly near the cutoff layer with a magnitude given by 1D geometric optics, provide the basis for a model of reflectometry that has been used in the past for the analysis of reflectometry data in the Tokamak Fusion Test Reactor (TFTR).[13,15] This model, which is reminiscent of that described in Ref. (16), appears somehow arbitrary and restrictive, but when valid it transforms microwave reflectometry into a practical tool for the investigation of short-scale turbulence in tokamaks. In the following, we will discuss the validity of this model of reflectometry using the results from a numerical solution of the wave equation in the presence of 2D turbulent fluctuations.

II. PHYSICAL MODEL

A. Plasma geometry

In the system of orthogonal coordinates (r,x) introduced in the previous Section, we consider a plane stratified plasma equilibrium with electron density $n_e(r)$. To make the numerical simulation more realistic, we use the density profile of Fig. 1, which is similar to the density distribution on the equatorial plane of a typical TFTR discharge. As in the standard reflectometry arrangement used in tokamaks, we assume that the probing wave is launched along the r-direction from the right side of Fig. 1, with its electric field perpendicular to the x-axis, corresponding to the ordinary mode of propagation in tokamaks. The wave frequency is $\omega/2\pi = 75 \times 10^9$ s^{-1} ($k_0 = 15.7$ cm^{-1}), and the radial position of the plasma cutoff is $r_c = 278$ cm, where the permittivity radial scale length is $L_\varepsilon = 50$ cm. For the density profile of Fig. 1, this cutoff position prevents any significant tunneling of the launched wave, which therefore must be completely reflected. Accordingly, we have used the total energy of reflected waves in the vacuum region as one of the tests for assessing the validity of our solution of the wave equation.

B. 2D Random fluctuations

Since the frequency of turbulent fluctuations in tokamaks is several orders of magnitude smaller than the frequency of the probing wave, we assume that the equilibrium plasma density $n_e(r)$ is perturbed by a spectrum of stationary random fluctuations with the amplitude distribution

$$\frac{\delta n_e}{n_e} = \sum_{p=1}^{M} \sum_{q=1}^{M} \delta_{pq} \cos(p\kappa_r r) \cos(q\kappa_x x + \varphi_{pq}), \tag{6}$$

which is composed of $M \times M$ discrete components with wavenumbers $p\kappa_r$ and $q\kappa_x$ (where κ_r and κ_x are constants), random phases φ_{pq}, and amplitudes δ_{pq}. For the latter, we take the distribution $\delta_{pq}^2 \propto p \exp[-(p\kappa_r/\Delta k_r)^2 - (q\kappa_x/\Delta k_x)^2]$ with $\Delta k_r = \kappa_r M/2$ and $\Delta k_x = \kappa_x M/2$. Without a loss of generality, we have introduced the factor p in the spectral distribution of fluctuations for simplifying the comparison of the numerical results with the predictions of Eq. (5), that can be obtained with a simple analytical integration in k_r. Such a factor is also justified by the fact that the focus in this paper is on short radial scale fluctuations.

C. Wave equation

We look for solutions of the wave equation in the form

$$E(x,r) = \sum_{n=-N}^{N} c_n E_n(x,r), \tag{7}$$

where $E_n(x,r)$ is a set of $2N+1$ independent solutions of the wave equation, which are cast in the form

$$E_n(x,r) = \sum_{m=-N}^{N} f_{mn}(r)e^{im\kappa_x x}, \tag{8}$$

so that the functions $f_{mn}(r)$ are solutions of the system of equations

$$\frac{d^2 f_{mn}}{dr^2} + k_0^2(\varepsilon_0 - \alpha_m^2)f_{mn} +$$
$$k_0^2(\varepsilon_0 - 1)\sum_{p=1}^{M}\sum_{q=1}^{M}[\frac{\delta_{pq}}{2}\cos(p\kappa_r r)(f_{(m-q)n}\,e^{i\varphi_{pq}} + f_{(m+q)n}\,e^{-i\varphi_{pq}})] = 0 \tag{9}$$

where $\varepsilon_0 = 1 - (\omega_p/\omega)^2$ is the unperturbed plasma permittivity, $\omega_p = (4\pi n_e e^2/m_e)^{1/2}$ is the plasma frequency, and $\alpha_m = m\kappa_x/k_0$. These equations, which are obtained by inserting Eqs. (6) and (8) into the wave equation and by performing a Fourier expansion in x, can be solved with the Runge-Kutta method. Then the coefficients c_n in Eq. (7) are determined by separating the electromagnetic field in the vacuum region into a forward and a backward component, and by imposing the condition that the former is a plane wave propagating in the r-direction with unit amplitude. In the vacuum region ($r > r_0$) the electromagnetic field can then be expressed in the form

$$E(x,r) = e^{-ik_0 r} + \sum_{n=-N}^{N} A_n e^{i[n\kappa_x x + (k_0^2 - n^2\kappa_x^2)^{1/2}r]}, \tag{10}$$

where the first term on the right hand side represents the launched wave, while the second represents the reflected waves, which in the following we will refer to as the backward field E_b. Finally, the value of the integer N is chosen so that an increase in its value does not significantly affect the solution. This condition, to be verified a posteriori, allows the closure of the system of Eqs. (9) by setting all terms $f_{(m\pm q)n}$ with $|m \pm q| > N$ to zero.

III. NUMERICAL RESULTS

The amplitude $|A_n|$ of reflected waves is shown in Fig. 2 as a function of $n\kappa_x$ for fluctuations with $\kappa_x=0.05$ cm^{-1}, $\kappa_r=0.1$ cm^{-1} and $M=20$. The three cases differ only in the value of the total density fluctuation, defined as the volume average $\sigma_n = <(\delta n)^2/n_e^2>^{1/2}$, which is equal to 5.0×10^{-3}, 1.0×10^{-2} and 2.0×10^{-2}, respectively. These results are a clear illustration of the broadening in the spectrum of backward waves and of the decrease in the amplitude of the specular reflection $|A_0|$, which are both caused by the rise in the amplitude of fluctuations.

Here and in the following, the phase $\phi(x)$ of E_b on a plane with a constant value of r is defined, apart from an additive constant, as the sum of the phase differentials between pairs of adjacent points. By setting their separation to be sufficiently small, one can avoid, with the exception of points where $|E_b| \approx 0$, the indetermination caused by the multivalued character of the phase.

For the same three cases of Fig. 2, Figs 3 and 4 displays the modulus $\rho \equiv |E_b|$ of the backward field, and the phase deviation from the mean value ($\tilde{\phi}$) at the plasma boundary $r=r_0$. From these results, it appears that the value of ρ fluctuates wildly as a result of the reflected waves interference, and thus that the backward field is far from being approximated by a plane wave. Also, since the density fluctuations of the three cases shown in Fig. 2 differ only by a constant factor, i.e., they have the same set of random phases δ_{pq}, the results in Fig. 4 show clearly that the calculated value of $\tilde{\phi}$ does not agree with the value obtained from Eq. (1), since the latter is approximately a linear function of $\delta n_e/n_e$. It is also interesting to note that as the amplitude of fluctuations increases the spectrum of $\tilde{\phi}(x)$ develops a strong low wavenumber component.

These results appear to suggest that the model of reflectometry described in the Introduction fails to predict the numerical results. Indeed this is not true. Suppose in fact, as done in our model, that the launched wave is nearly unaffected by plasma fluctuations up to a region near the cutoff where it then suffers a phase modulation. An observer in the vacuum region would detect a spectrum of reflected waves as if they were coming from a virtual location $r=r_G$, corresponding to the average round-trip group delay,[1] i.e., from $r \approx r_0 + \int_{r_0}^{rc} \varepsilon_0^{-1/2} \, dr$. For the case considered so far, we obtain $r_0 - r_G \approx 100$ cm. From the last term in Eq. (10), we get that the range of radial wavenumbers of the backward waves is

$\delta k_r \approx (1 + \sigma_\phi^2)\Delta k_x^2 / 2k_0$, where, as explained in the Introduction, the factor is due to the non-linear spectral broadening of scattered waves. Thus an observer, who is located at a distance from the plane $r = r_G$ which is larger than the *diffraction distance* $D = \delta k_r^{-1}$, would sample an electromagnetic field which is the result of a complicated interference pattern, and should therefore detect large amplitude variations and random phases, as those displayed in Figs. 3 and 4. For the case in Fig. 2 with the lowest level of fluctuations ($\sigma_n = 5.0 \times 10^{-3}$), we obtain $D \approx 60$ cm using the value of $\sigma_\phi \approx 1$ given by Eq. (1). Thus the results of Figs. 3 and 4 can be explained by the fact that $D < r_0 - r_G$ in all three cases of Fig. 2.

As a further clarification of these results, the variance $\sigma_E^2(r) \equiv \langle(\rho - \langle\rho\rangle_r)^2\rangle_r$ of the calculated backward field modulus (where $\langle \ \rangle_r$ indicates the average for constant value of r) is displayed in Fig. 5 as a function of r. The significance of this parameter is that can be approximated by the plane wave $\exp(i\tilde{\phi})$ whenever $\sigma_E \approx 0$. Figure 5 shows that in all three cases σ_E has an absolute minimum at $r = r_G$, but with a value which is a growing function of σ_n. As a result, while ρ is almost constant at $r = r_G$ for $\sigma_n = 5.0 \times 10^{-3}$ (Fig. 6), the case with $\sigma_n = 2.0 \times 10^{-2}$ displays large amplitude fluctuations at every radial location. As a point of reference, the dashed line in Fig. 5 represents the value of σ_E for a Gaussian noise where both the real and the imaginary parts are independent normal random variables with mean zero and variance 1/2. For such a field, the phase is uniformly distributed in the interval $(-\pi, \pi)$, and the modulus follows the Rayleigh distribution[17] $2\rho\exp[-\rho^2]$, which gives $\sigma_E^2 = 1 - \pi/4$. Thus from Fig. 5 we see that in all three cases, as one moves away from the plane $r = r_G$, the numerical value of σ_E^2 approaches the variance of a Gaussian noise.

As another test of our model, Fig. 7 compares the fluctuating component ($\tilde{\phi}$) of the phase of E_b at with the phase of geometric optics that is obtained by neglecting the bending of rays (Eq. (1)). This shows that, while in the first two cases of Fig. 2 the numerical value of $\tilde{\phi}$ is in excellent agreement with the predictions of 1D geometric optics, a substantial discrepancy occurs in the third case with $\sigma_n = 2.0 \times 10^{-2}$. As a matter of fact, since in the latter case $\sigma_n \approx (\Delta k_r L_\varepsilon)^{-1}$, even the phase of geometric optics displays large jumps because of the local inversions in the plasma permittivity.

In conclusion, these results show that the calculated backward field of case (*a*) in Fig. 2 is in good agreement with the predictions of our model. They also demonstrate how quickly such an agreement is

lost as the level of fluctuations increases. As mentioned in the previous paragraph, one of the conditions for the validity of our model must be

$$\sigma_n < \frac{1}{\Delta k_r L_\varepsilon} \ ,$$ (11)

which is required for avoiding discontinuities in the phase of geometric optics. Another condition can be derived with the following simple argument.[18] Since each spectral component of the backward field carries information from a region near its reflecting layer, the breakdown of our model must occur when the reflecting points are distributed over a distance Δr_c which is comparable to the radial wavelength of fluctuations, i.e., when $\Delta r_c \Delta k_r > 1$. Since the range of poloidal wavenumbers of reflected waves is $\approx \sigma_\phi \Delta k_x$ (see Introduction), we get $\Delta r_c / L_\varepsilon \approx \sigma_\phi^2 \Delta k_x^2 / k_0^2$, from which we obtain that one condition for the validity of geometric optics is

$$\sigma_\phi^2 < \frac{k_0^2}{L_\varepsilon \Delta k_r \Delta k_x^2} \ .$$ (12)

For the spectrum of density fluctuations used in this paper, Eqs. (5) and (6) give $\sigma_\phi^2 = \pi^{3/2} (k_0^2 L_\varepsilon / \Delta k_r) \sigma_n^2$, which allows Eq. (12) to be cast in the form

$$\sigma_n^2 < \frac{1}{\pi^{3/2} L_\varepsilon^2 \Delta k_x^2} .$$ (13)

From this we get $\sigma_n < 0.017$, which explains the failure of the model for the conditions of case (*c*) in Fig. 2. This criterion demonstrates the deleterious effects of 2D fluctuations with large values of Δk_x. To illustrate this phenomenon, Fig. 8 displays $|E_b|$ and $\tilde{\phi}$ at $r = r_G$ for the same conditions of case (*b*) in Figs. 6 and 7, but with twice the value of $\kappa_x (=0.1)$. From these results it is clear that, as predicted by Eq. (13), a rise in Δk_x causes an increase in the fluctuations of $|E_b|$, and a large discrepancy of the calculated value of $\tilde{\phi}$ with the phase of geometric optics.

The limit imposed by Eq. (11) is satisfied by the short-scale turbulence observed in tokamaks, since both theory and experiments indicate that the amplitude of fluctuations obeys the *mixing length criterion* $\sigma_n < 1 / \Delta k_r L_n$, where $L_n \approx L_\varepsilon$ is the density radial scale length. Thus a sufficient but not necessary condition for the validity of Eq. (13) is $\Delta k_r \geq \pi^{3/4} \Delta k_x$.

The results in Fig. 5 indicate that, for $r - r_G \geq D$, the variance of ρ approaches the value given by a Rayleigh distribution even in the case with the smallest level of fluctuation ($\sigma_n = 5.0\times10^{-3}$). Indeed, since such a distribution is characteristic of a Gaussian noise with $< E_b >_r = 0$, this seems to contradict our model of reflectometry which instead implies that, apart from a constant phase, $< E_b >_r \approx \exp(-\sigma_\phi^2 / 2) \neq 0$. To clarify this important point, we have performed a sample average over 32 realizations of the backward field, which were obtained by repeating the numerical calculation of E_b with a constant value of σ_n but different sets of the random phases φ_{pq} in Eq. (6). Figure 9 shows the average spectra of reflected waves for $\sigma_n = 2.5\times10^{-3}$ and $\sigma_n = 5.0\times10^{-3}$. From these, we can get a good estimate of the average value of $|A_0|$, which once inserted into the equation $|A_0| = \exp(-\sigma_\phi^2 / 2)$ gives $\sigma_\phi = 0.63$ and $\sigma_\phi = 1.17$ radian, respectively. We find that these values of σ_ϕ are in good agreement with the corresponding sample average of $< \tilde{\phi}^2 >_{r=r_G}^{1/2}$, for which we obtain 0.61 and 1.17, and with the similar average using the phase of geometric optics, which gives 0.61 and 1.18, respectively. Thus the separation of the backward field into a specular reflection and into a spectrum of scattered waves appears to be in excellent agreement with the prediction of our model. This suggests[19] that beyond the diffraction distance D, the statistical distribution of $|E_b|$ should be similar to the distribution derived by Rice for a sinusoidal signal in the presence of a Gaussian noise,[20,21] which is given by

$$F(\rho) = \frac{\rho}{\sigma^2} e^{-(\rho^2 + |A_0|^2)/2\sigma^2} I_0\left(\frac{\rho|A_0|}{\sigma^2}\right), \qquad (14)$$

where I_0 is the modified Bessel function of order zero, and σ^2 is the variance of both the real and the imaginary components of the noise. For the normalization used in this paper, we get $\sigma^2 = (1-|A_0|^2)/2$, and thus Eq. (14) becomes the Rayleigh distribution when $|A_0|=0$. Figure 10 shows the distribution of amplitudes at $r=500$ cm, calculated using the 32 realizations of the backward field, together with the Rice distribution corresponding to the values of $|A_0|$ in Fig. 9. These results demonstrate that Eq. (14) is indeed a good description of the distribution of amplitudes of the backward field. They also show that the Rayleigh distribution is not substantially different form the Rice distribution for $\sigma_n = 5.0\times10^{-3}$, which explains the apparent inconsistency of the results of Fig. 5 with the predictions of our model of reflectometry.

By now it should be clear that, even when our model of reflectometry is valid, the spectrum of turbulent fluctuations cannot be inferred from phase measurements in the far field region. As a another demonstration of this, for the conditions of case (*b*) in Fig. 9, Fig. 11 shows the power spectrum of $\tilde{\phi}$ at the cutoff virtual location ($r = r_G$), and at the plasma boundary ($r = r_0$). These results, which as before are obtained by averaging over 32 realizations of the backward field, show that the calculated power spectrum at $r = r_G$ is in good agreement with the spectrum of geometric optics, which is obtained from Eq. (5) by replacing the 1D spectrum $\Gamma_\varepsilon(k_r)$ with the corresponding 2D spectrum $\Gamma_\varepsilon(p\kappa_r, q\kappa_x)$ of Eq. (6), and by summing over the range of values of p. On the contrary, away from the cutoff virtual location, at a distance approximately equal to D, the bottom of Fig. 11 shows that the phase power spectrum tends towards a universal $1/k_x^2$ dependence, regardless of the spectrum of plasma fluctuations.

In conclusion, the numerical results presented in this paper appear to confirm a model of reflectometry where the reflection of waves from a plasma cutoff in the presence of 2D random fluctuations resembles the reflection of waves from a rough surface.[13,15,16] The validity of this model requires the amplitude of fluctuations to be smaller than a threshold value, which is determined by the spectrum of wavenumbers (Eqs. (11) and (13)). Once these conditions are satisfied, the backward field arises from a phase modulation of the probing wave, occurring mostly near the cutoff, with a magnitude given by 1D geometric optics. To an outside observer, the reflecting layer appears to be located behind the cutoff, at the radial location which corresponds to the average group delay. After reflection, the electromagnetic field separates into a wave propagating along the direction of specular reflection, and into a group of scattered waves propagating in different directions. The amplitude of the former decreases quickly to an insignificant level as the variance σ_ϕ^2 of the phase modulation becomes larger than one. At a distance from the cutoff virtual location, which is larger than the diffraction length $D \approx 2k_0 / (1 + \sigma_\phi^2)\Delta k_x^2$, the scattered waves produce a complicated interference pattern, which appears as a Gaussian noise.

These results emphasize the importance of performing the reflectometry measurements as close as possible to the virtual cutoff, since it is only by sampling the backward field at this location that it is possible to reconstruct the field of turbulent fluctuations. Experimentally, this could be achieved by collecting the reflected waves with a wide aperture antenna, and by imaging the virtual cutoff onto an array of phase sensitive detectors. A similar conclusion was reached in Ref. 7.

IV. DENSITY MEASUREMENTS

As a final application of our numerical simulations, we return to the problem of how to infer the plasma density profile from reflectometry measurements. As mentioned in the Introduction, this can be achieved using the frequency dependence of the round-trip group delay of a probing wave. The results presented in this paper are a clear illustration of the kind of difficulties that one may encounter in performing these measurement in the presence of 2D random fluctuations since, as shown in Fig. 4, even a small level of fluctuations can cause a complete randomization of the measured phase. It has been proposed that these difficulties could be circumvented by differential-phase measurements, employing two or more probing waves simultaneously. This can be achieved either by using the side bands produced by the amplitude modulation of a single wave,22,23 or by launching two waves with different frequencies.[24] The idea behind these proposals is that, if the distance between the cutoffs is sufficiently small, the effect of fluctuations can be compensated by averaging the differential phase. We have performed a numerical simulation of this type of measurements using two probing frequencies, and f_2, and the plasma conditions of case (b) in Fig. 2. Figure 12 shows the calculated phase difference $\Delta\phi = \phi_2 - \phi_1$ at $r = r_0$ for $f_1 = 74.8$ GHz and $f_2 = 75.0$ GHz, corresponding to a cutoff separation of $\Delta r_c = 0.26$ cm. A comparison of with the differential phase given by Eq. (1) in the absence of fluctuations indicates that it is indeed possible to obtain the average phase delay of geometric optics by averaging $\Delta\phi$. Unfortunately, this is not always the case, as it is demonstrated by Fig. 13, which shows the deleterious effects of a larger level of turbulence ($\sigma_n = 2.0 \times 10^{-2}$), or a broader spectrum of fluctuations ($\Delta k_x = 1.0$ cm^{-1}). In both cases, similarly to what is observed experimentally, the differential phase is dominated by large jumps, which make it difficult, if not impossible, to obtain the group delay by averaging $\Delta\phi$. These phase jumps are caused by a spatial decorrelation of the two signals, and they occur when the amplitude (ρ) of one of them becomes zero. These jumps would appear in the measurements of a two-frequency reflectometer as well, even though in this case the phase is measured along the r-axis. Such phase jumps cannot be compensated, as it is often stated erroneously, by increasing the sweep-rate of the probing frequencies. The remedy is instead a decrease in the frequency difference $\Delta f = f_2 - f_1$, as demonstrated by Fig. 14 which shows for =0.05 GHz. A further increase in the level of turbulence, or in the spectral width of fluctuations, results in the reappearance of the phase jumps, that again can be compensated by a further decrease

12

in Δf. Unfortunately, this process cannot continue when the differential phase of geometric optics becomes too small, so that it is no longer possible to get its value by averaging $\Delta\phi$.

In conclusion, our numerical simulations demonstrate the advantages of differential-phase measurements for inferring the density profile with microwave reflectometry, but they also indicate the serious limitations imposed by the presence of a small level of 2D random fluctuations.

ACKNOWLEDGMENT

REFERENCES

[1] V. L. Ginzburg, *The Propagation of Electromagnetic Waves in Plasmas*, (Pergamon Press, Oxford, 1964).

[2] J. Doane, E. Mazzucato, and G. Schmidt, Rev. Sci. Instrum. **52**, 12 (1981).

[3] A. Cavallo and R. Cano, Technical Report EUR-CEA-FC-1137 (Association EURATOM-CEA sur la Fusion, 1982).

[4] C. Laviron, in *Proceedings of the International Workshop on Diagnostics for ITER*, Varenna, 1995 (Plenum Press, New York, 1996), p. 107.

[5] E. J. Doyle, K. W. Kim, J. H. Lee, W. A. Peebles, C. L. Retting, T. L. Rhodes, and R. T. Snider, ibid., p. 117.

[6] M. Manso, D. Bartlett, L. Cupido, W. Kasparek, J. Sánchez, P. Stott, and D. Wagner, ibid., p. 133

[7] V. A. Vershkov, ibid., p. 143.

[8] E. Mazzucato, Bull. Am. Phys. Soc. **20**, 1241 (1975); Princeton Plasma Physics Report No. MATT-1151 (1975).

[9] M. L. Pitteway, Proc. Roy. Soc. A **252**, 556 (1958).

[10] E. Mazzucato and R. Nazikian, Plasma Phys. Controlled Fusion, **33**, 261 (1991).

[11] X. L. Zou, L. Laurent, and J. M. Rax, Plasma Phys. Controlled Fusion, **33**, 903 (1991).

[12] B. B. Afeyan, A. E. Chou, and B. I. Cohen, Plasma Phys. Controlled Fusion, **37**, 315 (1995).

[13] E. Mazzucato and R. Nazikian, Phys. Rev. Lett. **71**, 1840 (1993).

[14] M. Abramowitz and I. Stegun, Handbook of Mathematical Functions (Dover, New York, 1968).

[15] E. Mazzucato, S. H. Batha, M. Beer, M. Bell, R. E. Bell, R. V. Budny, C. Bush, T. S. Hahm, G. W. Hammett, F. M. Levinton, R. Nazikian, H. Park, G. Rewoldt, G. L. Schmidt, E. J. Synakowski, W. M. Tang, G. Taylor, and M. C. Zarnstorff, Phys. Rev. Lett., **77**, 3145 (1996).

[16] G. D. Conway, L. Schott, and A. Hirose, Rev. Sci. Instrum. **67**, 3861 (1996).

[17] A. Papoulis, *Probability, Random Variables, and Stochastic Processes* (McGraw-Hill Book Co., New York, 1965).

[18] E. Mazzucato and R. Nazikian, Rev. Sci. Instrum. **66**, 1237 (1995).

[19] R. Nazikian and E. Mazzucato, Rev. Sci. Instrum. **66**, 392 (1995).

[20] P. Beckmann and A. Spizzichino, *The Scattering of Electromagnetic Waves from Rough Surfaces* (The Macmillan Company, New York, 1963).

[21] S. O. Rice, Bell System Tech. J., **23**, 282 (1944); **24**, 96 (1945) (reprinted in N. Wax, *Selected Papers on Noise and Stochastic Processes* (Dover, New York, 1954)).

[22] V. A. Vershkov and V. A. Zhuravlev, Sov. Phys. Tech. Phys. **32**, 523 (1987).

[23] J. Sánchez, B. Braãnas, T. Estrada, de la Luna, and V. A. Zhuravlev, Rev. Sci. Instrum. **63**, 4654 (1992).

[24] G. R. Hanson, J. B. Wilgen, T. S. Bigelow, I. Collazo, and C. E. Thomas, Rev. Sci. Instrum. **63**, 4658 (1992).

FIGURE CAPTIONS

Fig. 1.   Electron density profile used in the simulation; r_c is the cutoff radial position for a wave propagating from the right side with $\omega/2\pi=75$ GHz and the ordinary mode.

Fig. 2.   Spectrum of backward waves as a function of $n\kappa_x$ for fluctuations with $\kappa_x=0.05$ cm^{-1}, $\kappa_r=0.1$ cm^{-1}, $M=20$, and $\sigma_n=5.0\times10^{-3}$ (a), $\sigma_n=1.0\times10^{-2}$ (b), $\sigma_n=2.0\times10^{-2}$ (c). Calculations were performed with $N=60$ (a), $N=70$ (b) and $N=90$ (c).

Fig. 3. $|E_b|$ vs. x at $r=r_0$ for the three cases of Fig. 2. The range of x is $2\pi/\kappa_x$

Fig. 4. $\tilde{\phi}$ vs. x at $r=r_0$ for the three cases of Fig. 2.

Fig. 5. σ_E as a function of r for the three cases of Fig. 2. Dashed line indicate the value of σ_E for a Gaussian noise.

Fig. 6.   Same as in Fig. 3 for $r=r_G$.

Fig. 7.   Same as in Fig. 4 for $r=r_G$; dashed line is the phase of geometric optics .

Fig. 8. $|E_b|$ and $\tilde{\phi}$ vs. x at $r=r_G$ for the conditions of case (b) in Fig. 2, but with $\kappa_x=0.1$ cm^{-1}; dashed line is the phase of geometric optics.

Fig. 9.   Sample average of the backward field spectrum; (a): $\sigma_n=2.5\times10^{-3}$, $N=40$; (b): $\sigma_n=5.0\times10^{-3}$, $N=60$. Other parameters are the same as in Fig. 2.

Fig. 10. Amplitude distribution of the backward field at $r=500$ cm for the two cases of Fig. 9 (solid line). Dash-line is the Rician distribution; dot-line is the Rayleigh distribution.

Fig. 11. Phase power spectrum of backward field at $r=r_G$ (top) and $r=r_0$ (bottom). Conditions are those of case (b) in Fig. 9. Circles are from Eqs. (5) and (6).

Fig. 12. Differential phase $\Delta\phi$ at $r=r_0$ for $\Delta f=0.2$ GHz. Fluctuations are the same as in case (b) of Fig. 2. The dashed line represents the value of $\Delta\phi$ of geometric optics in the absence of fluctuations.

16

Fig. 13. Same as in Fig. 12, but with $=2.0\times10^{-2}$ (top), and $\Delta k_x=1.0$ cm^{-1} (bottom).
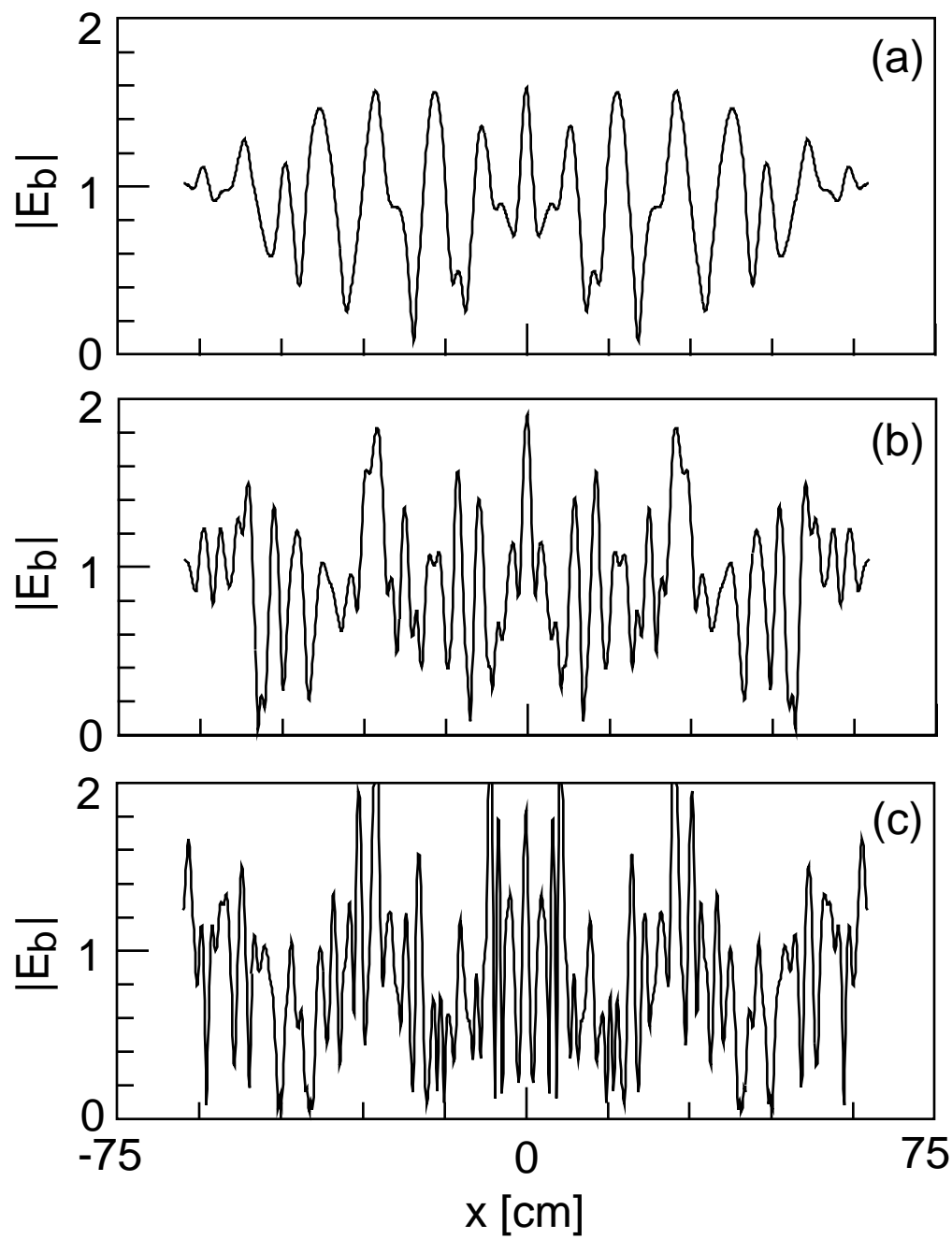
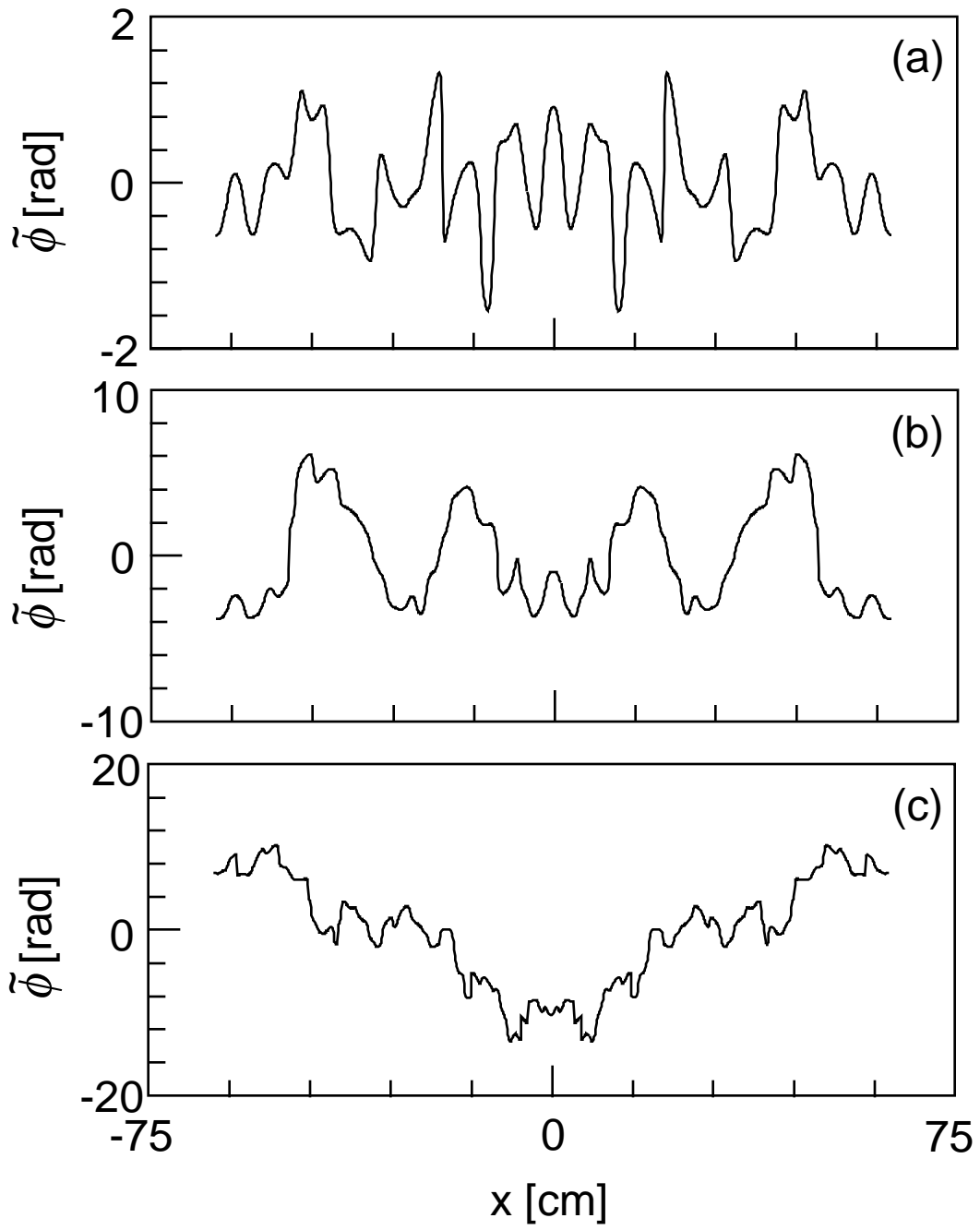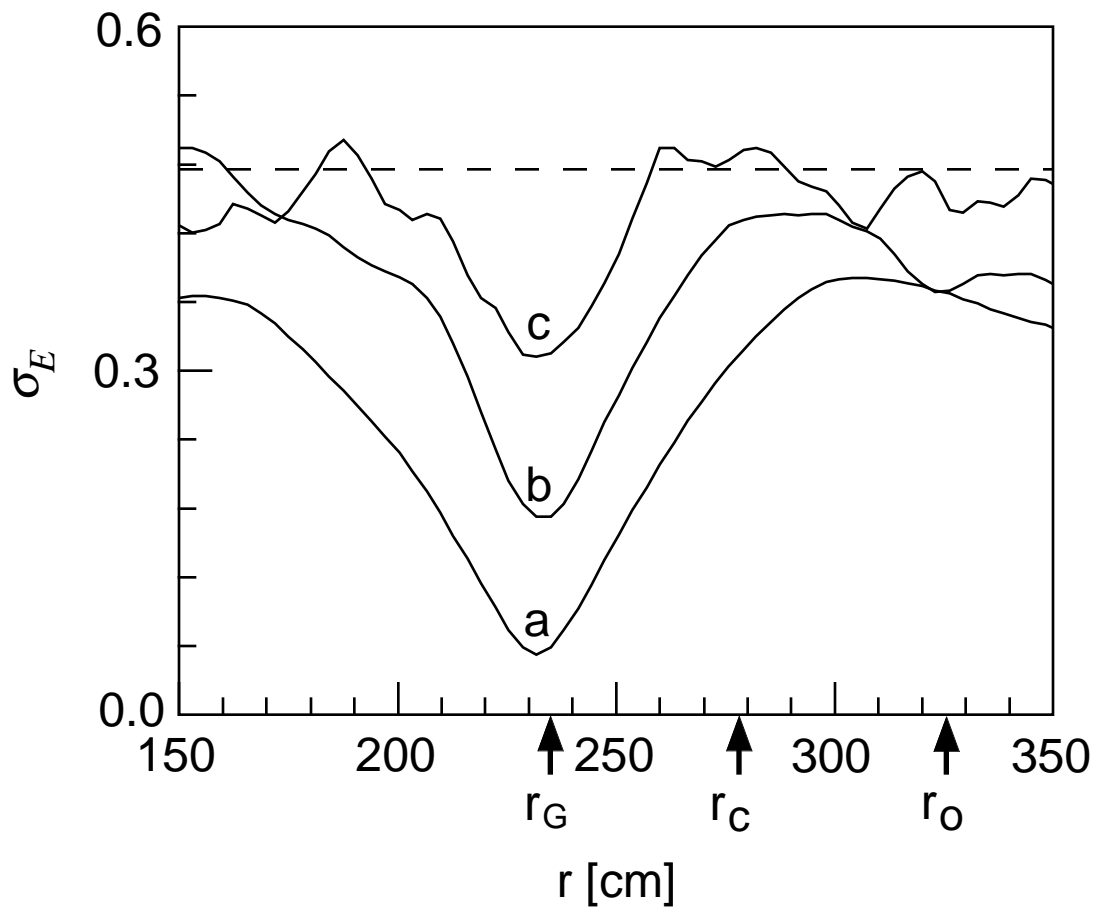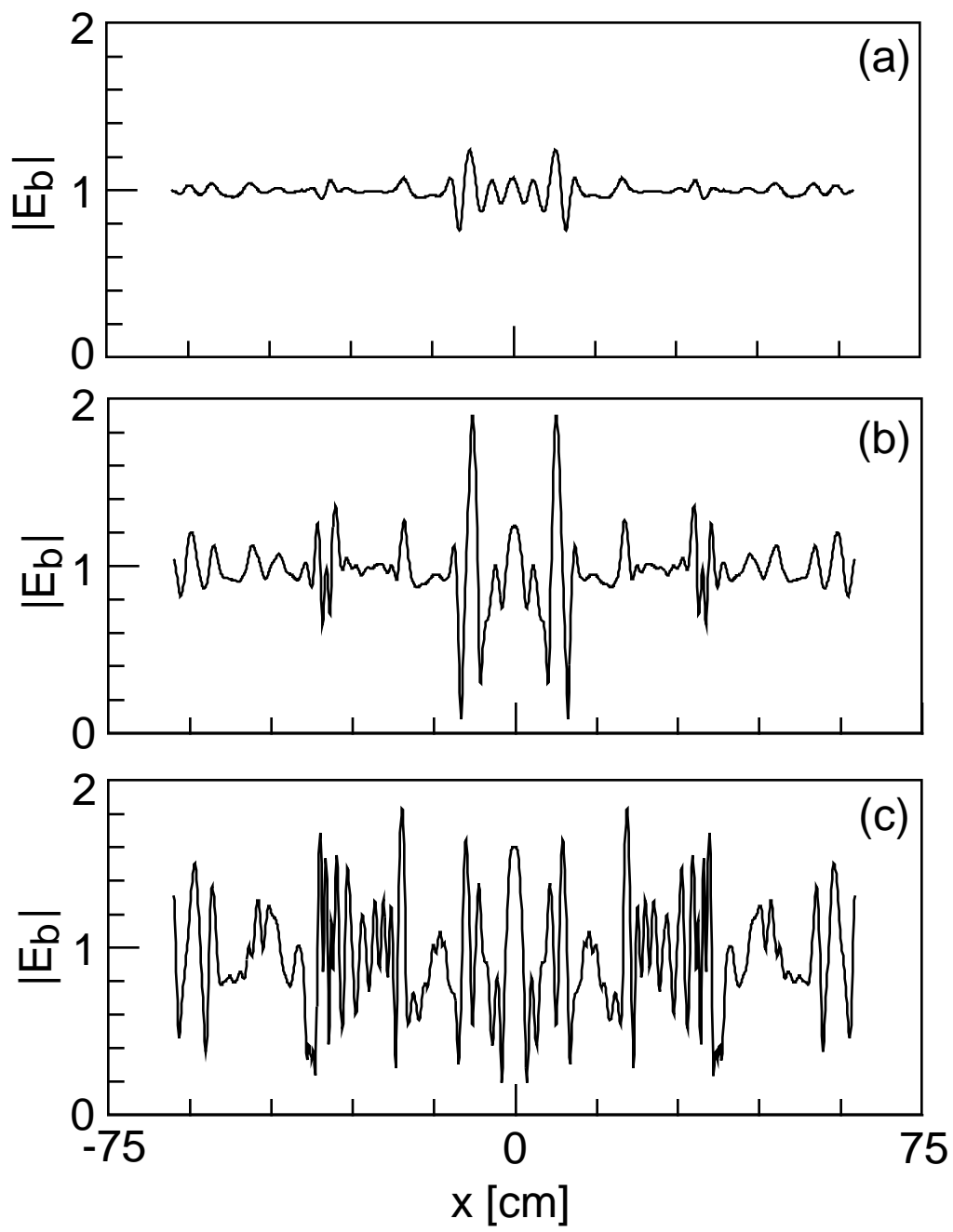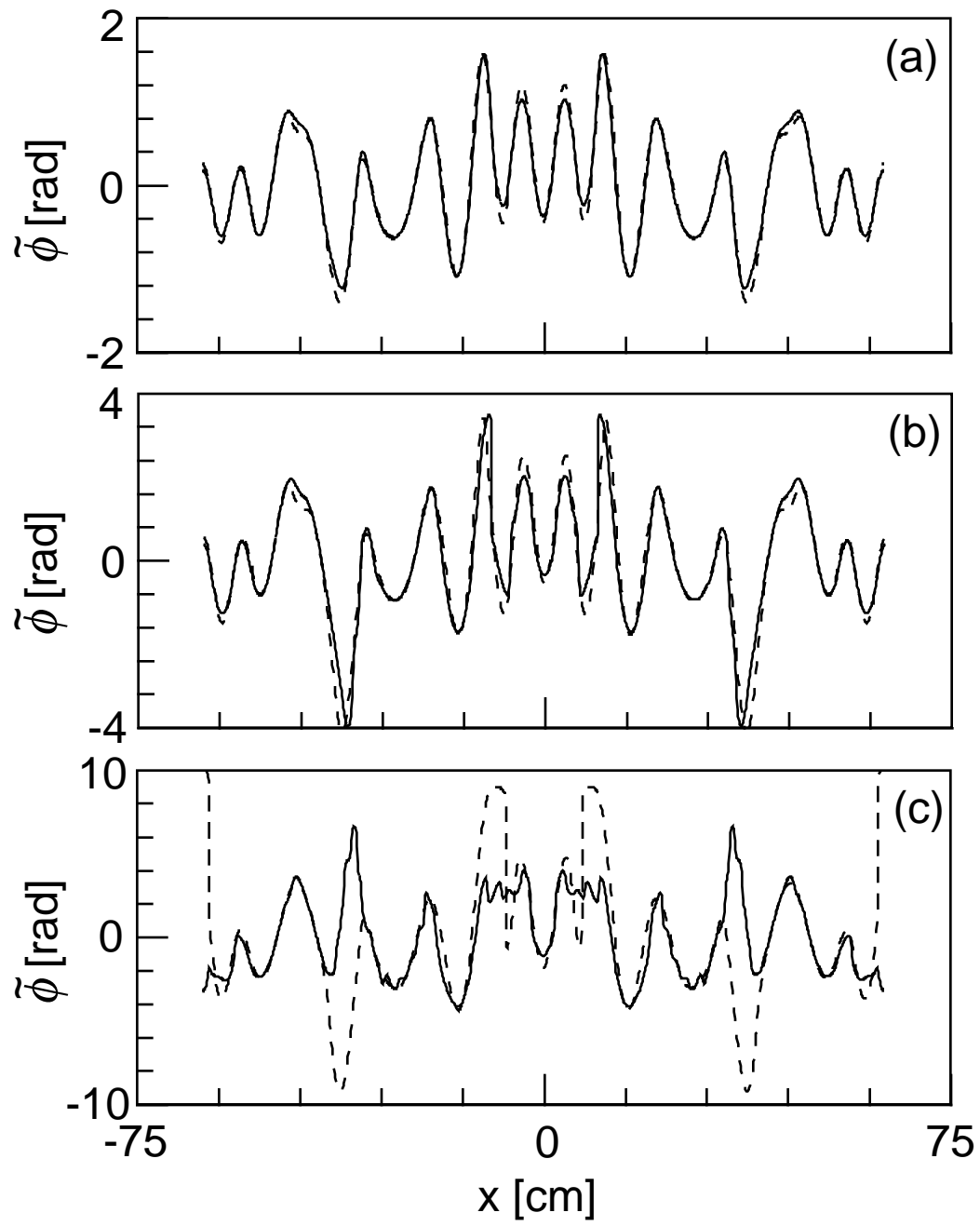Fig. 14. Same as in Fig. 13, but with $\Delta f=0.05$ GHz.
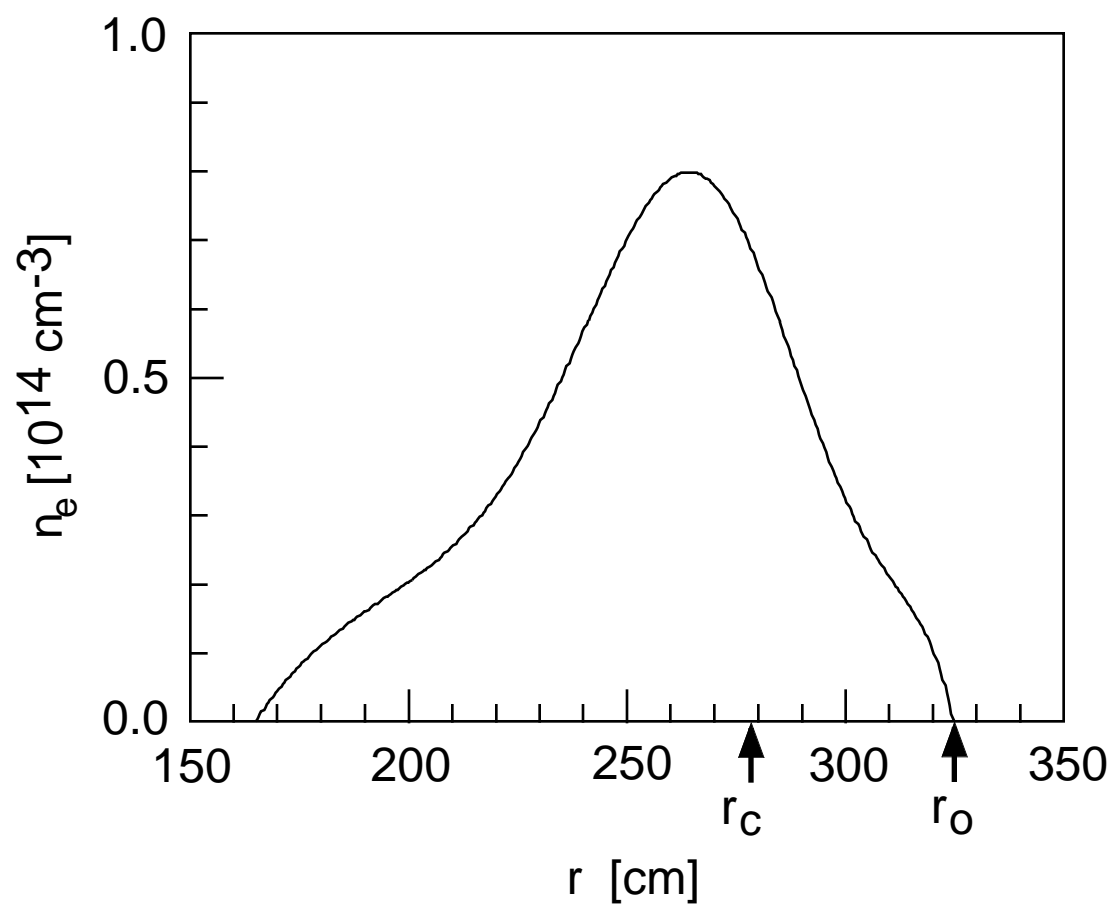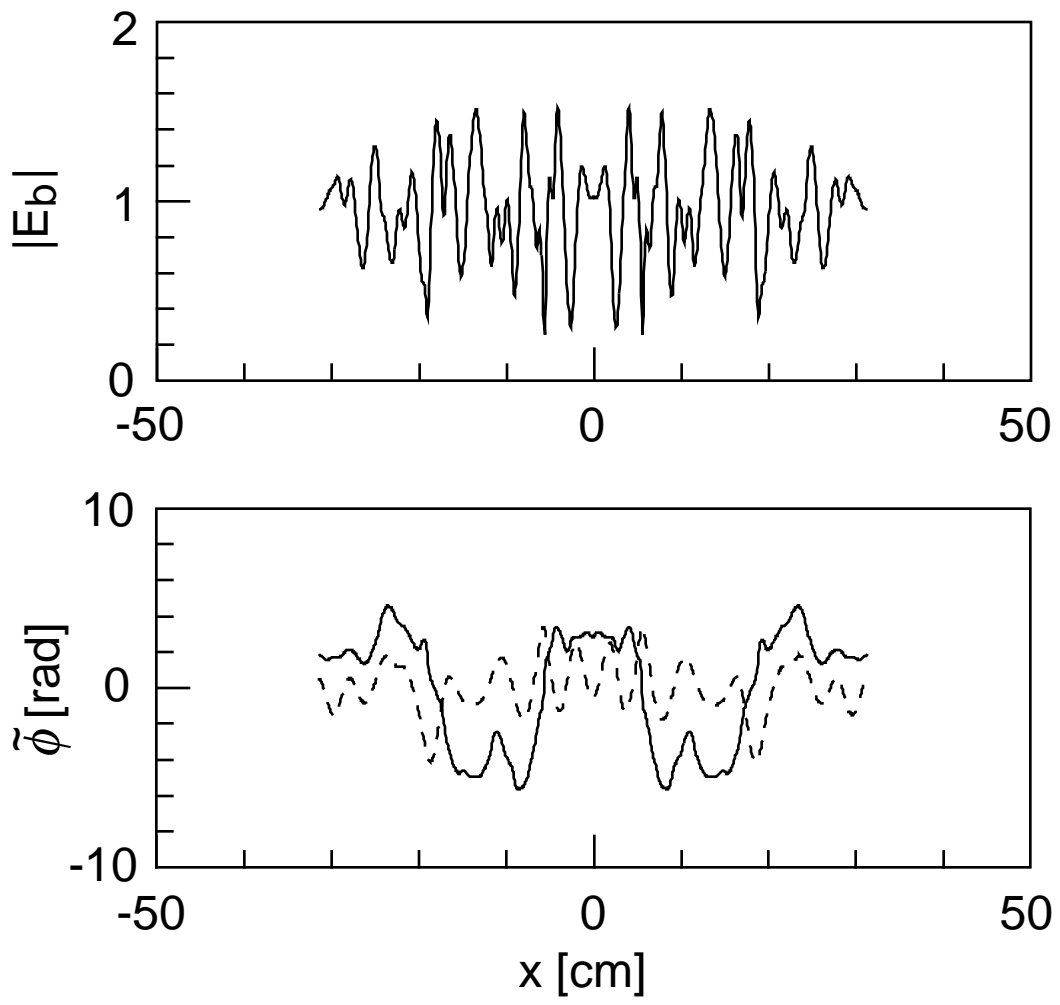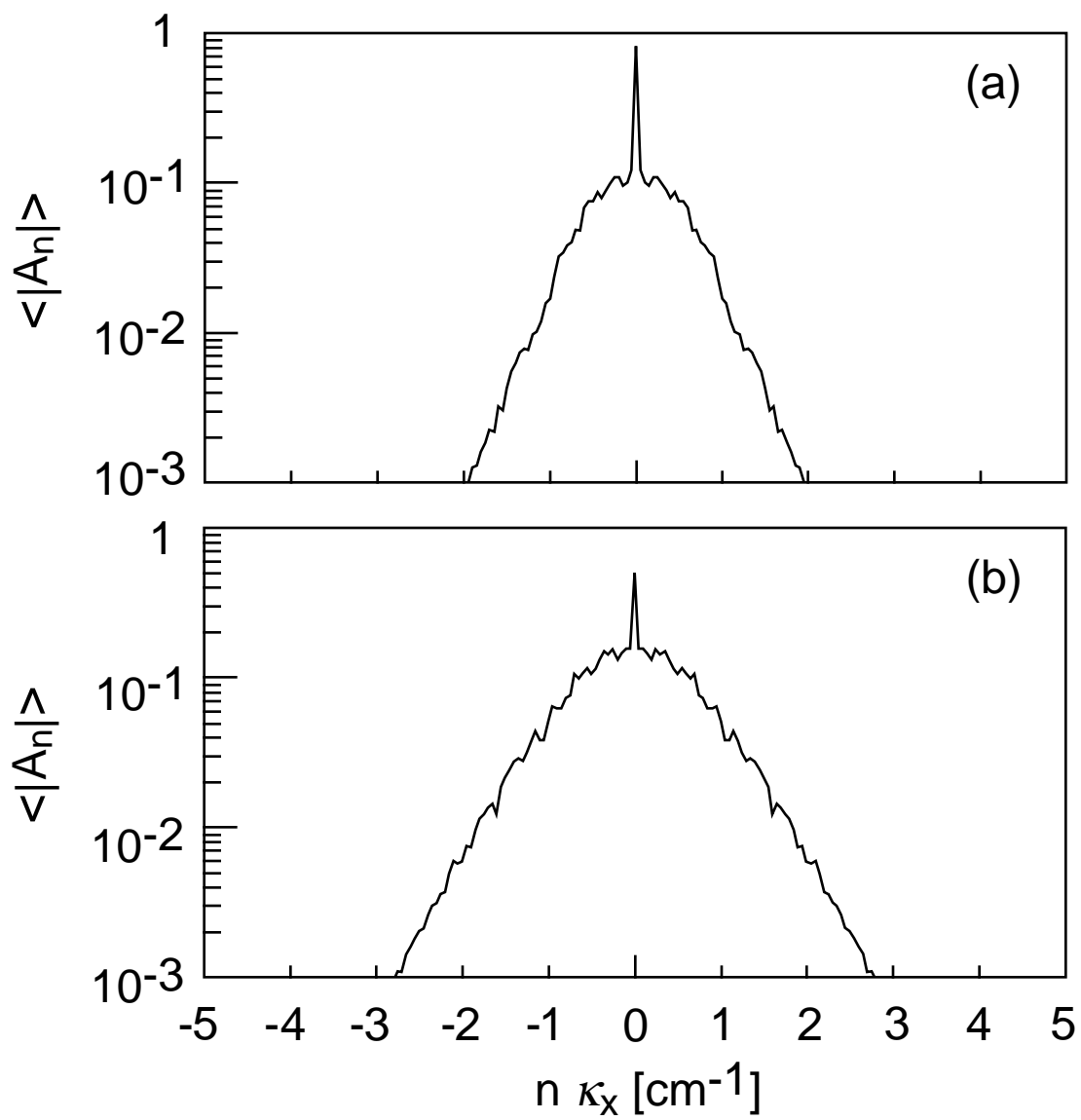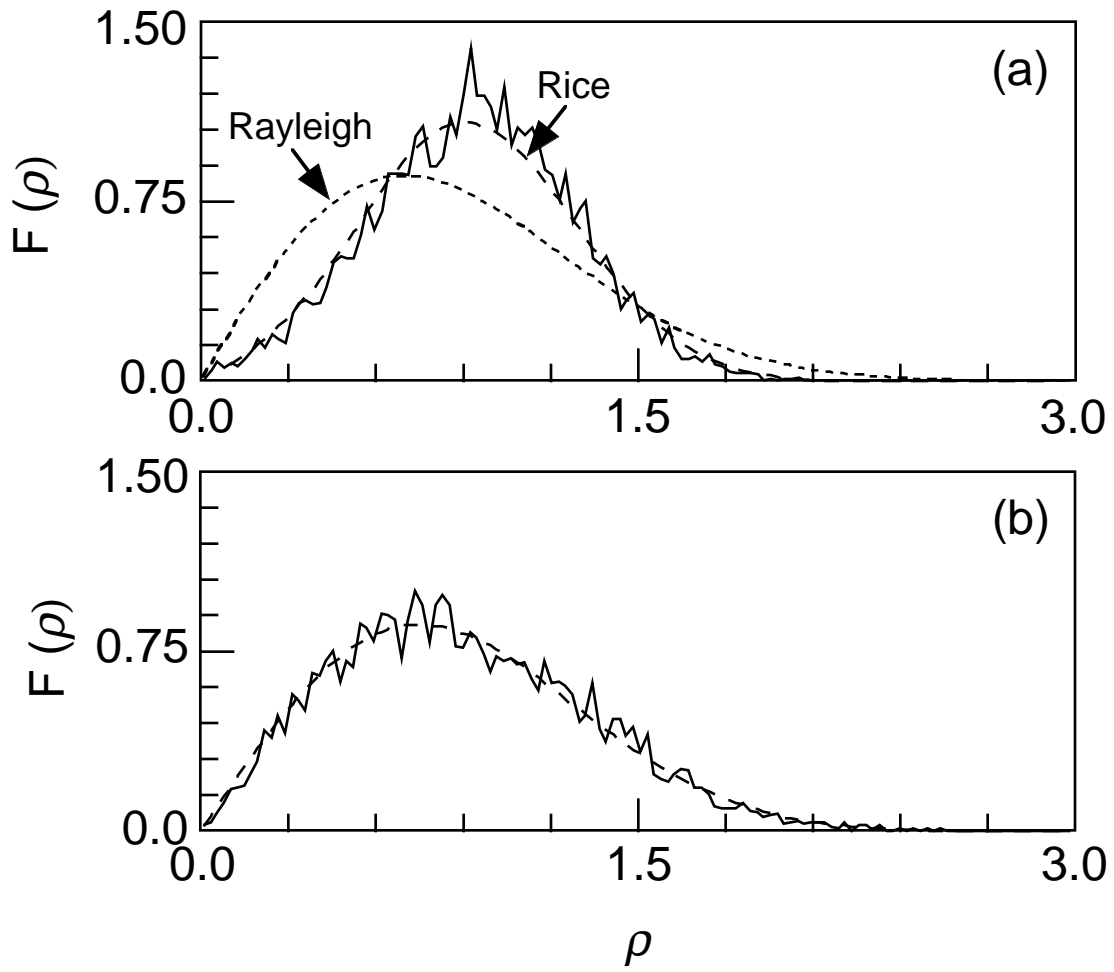
Fig. 1
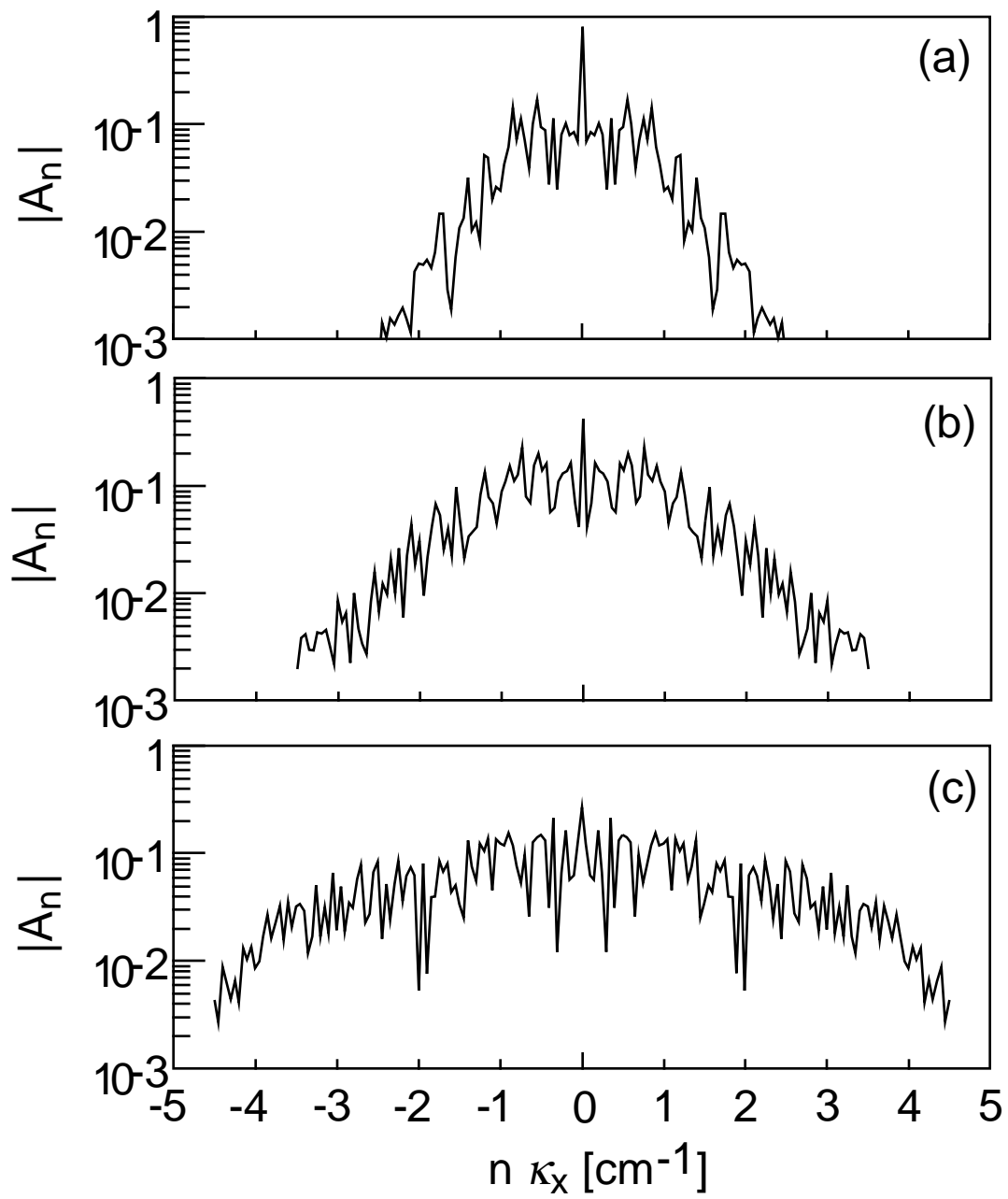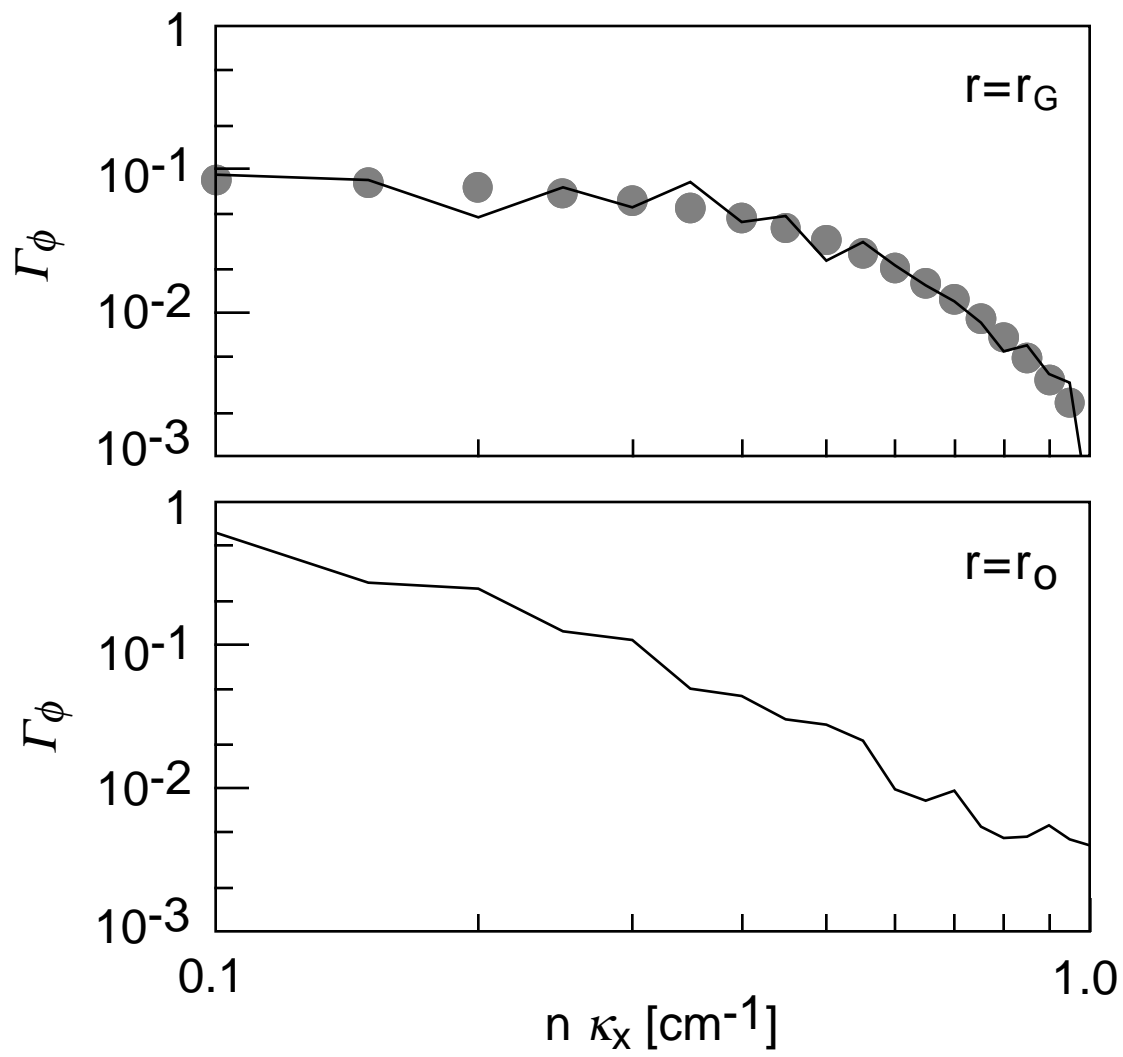
Fig. 2

Fig. 3

Fig. 4

Fig. 5

Fig. 6

Fig. 7

Fig. 8

Fig. 9

Fig. 10

Fig. 11

Fig. 12

Fig. 13

Fig. 14